Journal of Catalysis **200,** 140–147 (2001)
doi:10.1006/jcat.2001.3189, available online at http://www.idealibrary.com on IDEAL®

Synthesis and Activity of a New Catalyst for Hydroprocessing: Tungsten Phosphide

Paul Clark, Wei Li, and S. Ted Oyama[1]

Environmental Catalysis and Materials Laboratory, Department of Chemical Engineering (0211), Virginia Polytechnic Institute and State University, Blacksburg, Virginia 24061

Received October 19, 2000; accepted January 29, 2001; published online April 11, 2001

A tungsten phosphide, WP, hydrotreating catalyst was prepared by temperature-programmed reduction of an X-ray amorphous tungsten phosphate at a heating rate of 0.0167 K s^{-1} and a 2-h soak at the final temperature of 938 K. Characterization of intermediates quenched at different temperatures revealed a single crystalline reaction product whose specific CO uptake and BET surface areas passed through a maximum of 12 μmol g^{-1} and 15 m^2 g^{-1}, respectively, at 873 K. Heating rate variation measurements gave an apparent first-order activation energy of 148 kJ mol^{-1} for the reduction. Tungsten phosphide was catalytically active in the hydrodenitrogenation and hydrodesulfurization reactions of a simulated light oil consisting of 20 wt% tetralin, 76 wt% tetradecane, 2000 wppm N as quinoline, 3000 wppm S as dibenzothiophene, and 500 wppm O as benzofuran. Measurements were made in an upflow fixed-bed reactor operated at 3.1 MPa and 643 K and gave conversion levels at steady state for the WP catalyst of 58% HDN and 67% HDS. These conversions were superior to those found for WC, W_2N, and WS_2 tested under the same conditions.

Key Words: **tungsten; phosphide; sulfide; hydrodenitrogenation (HDN); hydrodesulfurization (HDS); quinoline; dibenzothiophene.**

INTRODUCTION

There has been considerable recent interest in the development of new hydroprocessing catalysts because more efficient conversion of heavier oil fractions is becoming increasingly important as world petroleum reserves are consumed and lower quality base stocks are utilized. Hydrodenitrogenation (HDN) is the most desired reaction in first-stage hydrocracking of heavy oil fractions such as vacuum gas oils (1), preparing the liquid for cracking over acid catalysts which are poisoned by nitrogen bases. Typical hydroprocessing catalysts are alumina-supported bimetallic sulfides of molybdenum or tungsten with either nickel or cobalt "promoter" (2–4) and often contain phosphorus as a secondary promoter (5–10).

[1] To whom correspondence should be addressed. E-mail: oyama@vt.edu.

Recent developments in hydroprocessing catalysis include the introduction of novel carbide and nitride compositions (11–13), the use of sulfides of early transition metals (14–17), the use of noble metals (18–20), and the use of zeolites (21, 22).

This study describes the synthesis and characterization of a new catalytic material, tungsten phosphide, which has high activity for hydroprocessing. The cata lyst is a member of a class of compounds known as the transition metal phosphides, with metallic or semiconducting properties and physical characteristics typical of intermetallic compounds. There are only a few reports of the use of transition metal phosphides as heterogeneous catalysts. Ni_2P and other phosphides have been applied as olefin hydrogenation catalysts (23–25), and bulk Ni_2P and Co_2P were found to be active for denitrogenation of quinoline (26). Amorphous nickel phosphide prepared by chemical reduction of nickel acetate and sodium hypophosphate with sodium borohydride is active for the hydrogenation of nitrobenzene to aniline (27). Recently, molybdenum phosphide was reported to be an active and stable HDN catalyst as well (28, 29). Molybdenum nitride prepared from Mo-P heteropolycompounds showed good activity for the hydrodesulfurization of benzothiophene (30, 31), but deactivated in the HDN of indole (32). The phosphorus in the nitrided compounds was stated to be in the form of phosphate combined with Mo (32), although X-ray photoelectron spectroscopy showed a small amount of phosphide (31).

Bulk tungsten compounds which have been previously reported as hydroprocessing catalysts include the sulfide WS_2 (3, 4), carbide WC (13), and nitride W_2N (33, 34). Pure WS_2 samples with high specific surface area are typically prepared by decomposition of ammonium tetrathiotungstate (35–38). High surface area tungsten carbide and nitride samples are obtained by temperature-programmed reactions of WO_3 with methane/hydrogen and ammonia, respectively. The tungsten phosphide, WP, used in this study was prepared by the direct hydrogen reduction of a stoichiometric phosphate glass at moderate temperature.

0021-9517/01 $35.00

Phosphorus is commonly used a secondary promoter in commercial hydroprocessing catalyst formulations (5, 8–10). In these catalysts phosphorus is introduced onto the alumina support by aqueous impregnation and is in the form of an oxide or phosphate on the surface. This is the first report of the synthesis and characterization of a tungsten phosphide hydroprocessing catalyst, where the phosphorus is found in the reduced form in the bulk.

EXPERIMENTAL

The starting material for the synthesis of tungsten phosphide was a tungsten phosphate. The phosphate was prepared by combining stoichiometric quantities of ammonium metatungstate, $(NH_4)_6W_{12}O_{39} \cdot xH_2O$ (Aldrich), and ammonium phosphate, $(NH_4)_2HPO_4$ (Aldrich, 99%), in sufficient distilled water to form a clear solution. Then the solution was evaporated to dryness and calcined in air at 773 K for 6 h. The product, tungsten phosphate, was ground to a powder with a mortar and pestle for further use.

Tungsten phosphide, WP, was prepared from the tungsten phosphate precursor by means of temperature-programmed reduction (TPR) with linear temperature ramps in flowing hydrogen. In the TPR procedure, which was used to identify the reduction characteristics of the material, 0.300 g of material was loaded in a quartz glass u-tube reactor and the effluent was monitored by a mass spectrometer (Ametek/Dycor MA100). In catalyst preparation, larger batches using up to 1.50 g of tungsten phosphate were prepared and combined to form the working WP catalyst. For the WP catalyst, the temperature was increased to 938 K at 0.0167 K s^{-1}, where it was held for 2 h before quenching in helium flow (67 μmol s^{-1}). The flow rate of hydrogen was maintained at 650 μmol s^{-1} g^{-1} starting material (300 cm^3(NTP) min^{-1} for 0.300 g metal phosphate) in all experiments.

Tungsten sulfide, WS_2, was prepared by decomposition of ammonium tetrathiotungstate, $(NH_4)_2WS_4$ (Aldrich, 99.9 + %), in a 10% H_2S/H_2 mixture. The sample was prepared from three batches of 1.3 g of ammonium tetrathiotungstate heated at 0.0833 K s^{-1} in 870 μmol s^{-1} of 10% H_2S/H_2 to a final temperature of 678 K, which was held for 2 h. Sulfur precipitated in the exit of the reactor tube during this process. The syntheses of the high surface area WC and W_2N have been described in the literature (12, 13, 33, 34).

The WP samples were passivated progressively with 0.1% O_2/He (80 μmol s^{-1} for 12 h), 0.5% O_2/He (13 μmol s^{-1} for 2 h), followed by diffusive air exposure in the reactor tube for 24 h, before collection and storage. All gases were supplied by Air Products. The listed purity of hydrogen, helium, and carbon monoxide was 99.999%, and that of oxygen was 99.99%. These gases were passed through a water trap (Alltech) before contacting the samples. Specialty mixtures, including 0.5% O_2/He, 30% N_2/He, and 10% H_2S/H_2 were used as received.

Chemisorption (CO uptake, O_2 uptake) and single-point BET surface area measurements were performed on samples directly after preparation, immediately after cooling to room temperature in helium, and are referred to here as *in situ* measurements. Characterizations performed on passivated, air-exposed samples rereduced in hydrogen for 2 h at 623 K, were used as the basis for hydroprocessing tests and are referred to in this report as *ex situ* measurements. Pulses (5.6 μmol) of CO at room temperature (300 K) or O_2 at dry ice/acetone temperature (195 K) were passed over the sample to measure the total, dynamic gas uptake. Single-point BET surface area measurements were carried out by passing a 30% N_2/He gas mixture to the sample at liquid nitrogen temperature and then measuring the nitrogen desorbed as the sample was heated rapidly to room temperature.

X-ray diffraction (XRD) spectra were collected using a Scintag XDS-2000 X-ray diffractometer using Ni-filtered Cu$K\alpha$ ($\lambda = 0.1541$ nm) radiation and a scan rate of $0.035^\circ 2\theta s^{-1}$. Crystallite sizes were estimated from the XRD peak line-widths using the method of Scherrer (39). The activation energy was calculated for the reduction reaction by the heating rate variation method of Redhead (40).

X-ray photoelectron spectroscopy (XPS) experiments were performed with a Perkin- Elmer 5000 surface analyzer on samples exposed to the atmosphere and not sputtered. Samples were mounted on double-sided adhesive tape, and binding energies were referenced to adventitious carbon at 285.0 eV. Quantification was achieved using sensitivity factors published by the instrument manufacturer (41).

Hydrotreating was carried out at 3.1 MPa (450 psig) and 643 K (370°C) in a three-phase upflow fixed-bed reactor operated as described previously (4). The feed liquid was prepared by combining tetralin (Aldrich, 99%), tetradecane (Fisher, 99%), quinoline (Aldrich, 99%), dibenzothiophene (Aldrich, 99%), and benzofuran (Aldrich, 99%) to create a liquid with composition summarized in Table 1. The liquid was delivered to the catalyst at 8.33×10^{-5} $dm^3 s^{-1}$ (5 $cm^3 min^{-1}$) along with 100 μmol s^{-1} (150 cm^3 (NTP) min^{-1}) hydrogen flow. Liquid product compositions

TABLE 1

Composition and Delivery Rates of Model Oil

Component	mol%	wt%	N, S, O (wppm)	Delivery rate (μmol h^{-1})
Quinoline	2.6	1.9	2000	580
Dibenzothiophene	1.7	1.7	3000	380
Benzofuran	0.6	0.4	500	130
Tetralin	27	20	0	6,100
Tetradecane	68	76	0	15,500

were determined with a Hewlett Packard 5890A gas chromatograph, equipped with a 50-m dimethylsiloxane column having 0.3 μm i.d. and 0.2 μm film thickness (Chrompack, CPSil 5B), on samples collected at 2- to 3-h intervals.

For the hydroprocessing reaction, the passivated WP catalyst was pretreated for 2 h at 623 K in 100 μmol s^{-1} (150 sccm NTP) of H_2, at a pressure slightly above 1 atm. The WS_2 catalyst was pretreated at 578 K for 2 h under 100 μmol s^{-1} of 10% H_2S/H_2. After the catalyst pretreatment, the reactor temperature and pressure were set to reaction conditions, and the liquid flow was started. Steady state was verified to be obtained in the last 30 h of a 60+-h reaction run. In this report, % HDN is defined as the total conversion of quinoline minus the sum of nitrogen containing products, % HYD is the sum of N containing quinoline intermediates (as no S containing hydrogenated intermediates were observed), and % HDS is defined as the conversion of dibenzothiophene.

RESULTS

Synthesis of Tungsten Phosphide

A typical reduction profile of the reaction forming tungsten phosphide is presented in Fig. 1, along with *in situ* characterization results from quenched intermediate samples. A small amount of water of hydration is evolved near 373 K; otherwise, there is only a single reaction peak produced by the reduction process. The *in situ* surface areas and CO chemisorption values shown in Fig. 1 increase with temperature up to 893 K, then begin to decrease. The trends in these properties follow the water evolution profile.

X-ray diffraction spectra of the quenched and passivated intermediates noted in Fig. 1 are shown in Fig. 2. The starting material is amorphous and unchanged at 773 K. The single product of the reaction, WP, grows in smoothly as the reaction progresses. Tungsten phosphide adopts the orthorhombic manganese phosphide (MnP) structure type (strukturbericht designation B31; space group *Pbnm*), a structure which is closely related to the hexagonal NiAs structure type (42, 43), but in which lattice distortions accompany the formation of chains of phosphorus atoms (44). The lattice parameters for WP are $a_o = 0.6219$ nm, $b_o = 0.5717$ nm, and $c_o = 0.3238$ nm (45). An estimation of the surface site density is made based on the lowest index planes as follows. We find 2 atoms per cell in the (100) plane, leading to 0.0926 nm^2 per W atom, 2 atoms per cell in the (010) plane, giving 0.1007 nm^2 per atom in this plane, and 3 atoms per cell in the (001) plane, yielding 0.1185 nm^2 per W. The average is then calculated to be 0.1037 nm^2 per W, which is similar to the value of 0.103 nm^2 (10.3 $Å^2$) per Mo reported by Stinner *et al.* (29) for MoP.

Variation of the heating rate in WP synthesis from 0.00833 to 0.0833 K s^{-1} (i.e., over an order of magnitude) shifted the temperature maximum as noted in Table 2. From

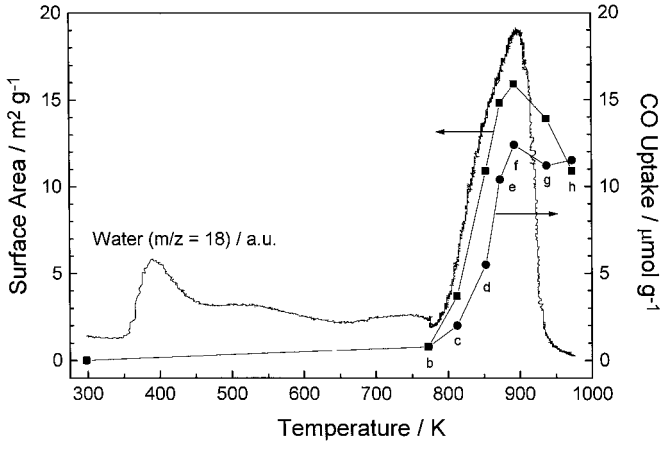

FIG. 1. Water evolved during the synthesis of tungsten phosphide from tungsten phosphate glass. Samples were preheated to 773 K at 0.0833 K s^{-1} and then ramped at 0.0167 K s^{-1} to their final temperature. *In situ* surface area (■) and CO uptake values (●) of quenched intermediates are compared to the reaction progress. The letters b–h also correspond to XRD spectra of quench intermediate samples noted in Fig. 2.

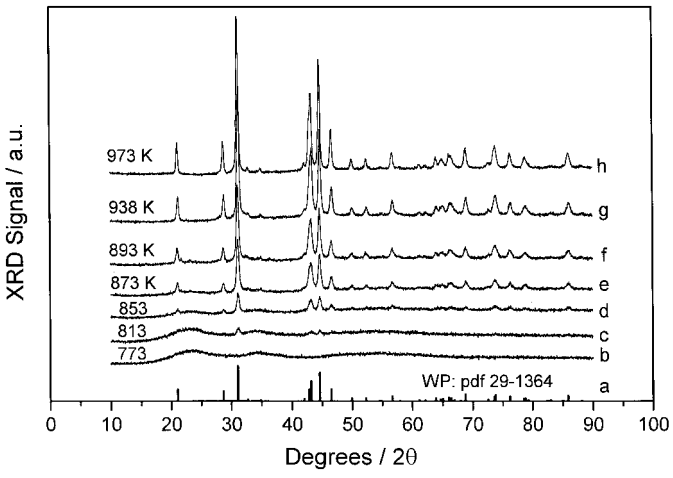

FIG. 2. X-ray diffraction patterns of intermediate samples quenched at various temperatures after reduction in hydrogen at 0.0167 K s^{-1}. The letters b–h also correspond to BET surface area and CO chemisorption values of intermediate samples noted in Fig. 1.

TABLE 2

Peak Temperature in the Formation of WP as a Function of Heating Rate

Heating rate (K min^{-1})	Temperature maximum (K)
0.5	862
1	893
2	934
3	952
5	1013

TABLE 3

Comparison of *ex Situ* Measurements of Surface Area, CO Chemisorption, and Site Density Characteristics of WP Catalyst, before and after Hydrotreating Study

Sample	BET surface area ($m^2\ g^{-1}$)	CO uptake ($\mu mol\ g^{-1}$)	Site density (site cm^{-2})
Fresh WP	10	10	6×10^{13}
Spent WP	11	11	6×10^{13}

this data, a first-order activation energy of 148 kJ mol^{-1} is calculated for the reduction process.

Catalyst Characterization

The WP catalyst was characterized before and after the hydroprocessing reaction by *ex situ* (defined above) BET surface area determination, *ex situ* CO chemisorption, and X-ray diffraction. The surface area and CO chemisorption characteristics of the catalyst are reported in Table 3, and the XRD spectra are shown in Fig. 3. These characteristics were effectively unchanged by catalytic reaction, and the results demonstrate that the WP bulk and surface are stable under reaction conditions. That the bulk WP phase is not altered by reaction is also verified by the stability of the lattice parameters and crystallite size (in the [011] directions) as reported in Table 4. The fresh tungsten sulfide catalyst had *ex situ* BET surface area of 37 $m^2\ g^{-1}$ and O_2 uptake of 58 μmol O g^{-1}.

Catalytic Reaction

The tungsten phosphide catalyst was used as a powder, rereduced in the hydroprocessing reactor at 723 K for 2 h. Tungsten sulfide was also used as a powder, but was dispersed in quartz chips and presulfided at 678 K. Amounts of catalysts corresponding to 30 m^2 were loaded in each catalytic reaction. Quinoline HDN and dibenzothiophene HDS activities of tungsten phosphide are presented in Fig. 4 as a function of time on stream. The HDN conversion is stable with time, averaging 58% during the last 30 h of reaction. The HDS conversion ranges between 55 and 60% until 30 h and then increases to near 67% for the final 30 h of reaction.

TABLE 4

Summary of XRD Results for Tungsten Phosphide Catalyst before and after Reaction

Lattice parameter	Fresh WP (nm)	Spent WP (nm)	Reference WP[a] (nm)
a	0.573	0.573	0.573
b	0.325	0.325	0.325
c	0.624	0.623	0.622
Crystallite size			
d_{011} (nm)	246	246	
S_{011} (m^2/g^{-1})	20	20	

[a] *pdf* 29–1364.

The estimated product distributions from the individual hydroprocessing reactions are reported elsewhere for the WP and WS_2 catalysts (46). The total analysis is complex as there were over 60 molecules detected in each GC trace. Values reported in parentheses are selectivity percentages for products, and conversions for reactants. Quinoline reaction proceeded on WP with formation of hydrogenated products 1,2,3,4-tetrahydroquinoline (10%), 5,6,7,8-tetrahydroquinoline (13%), and *ortho*-propylaniline (5%). The primary hydrocarbon products of quinoline HDN were propylcyclohexane (29%) and propylbenzene (16%). The products identified from dibenzothiophene HDS were biphenyl and cyclohexylbenzene. The WP

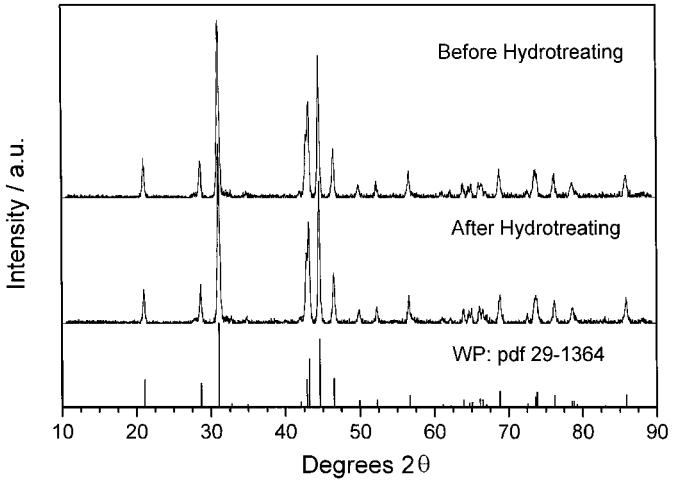

FIG. 3. X-ray diffraction patterns of the WP catalyst before and after reaction.

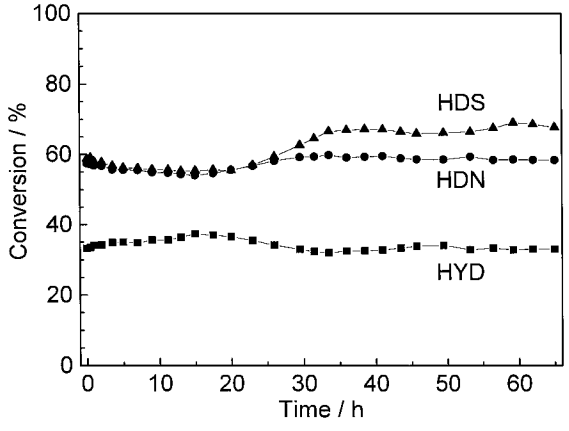

FIG. 4. Hydrotreating performance of tungsten phosphide with time. HDS, dibenzothiophene conversion; HDN, quinoline conversion minus HYD; and HYD, sum of anilines and tetrahydroquinolines.

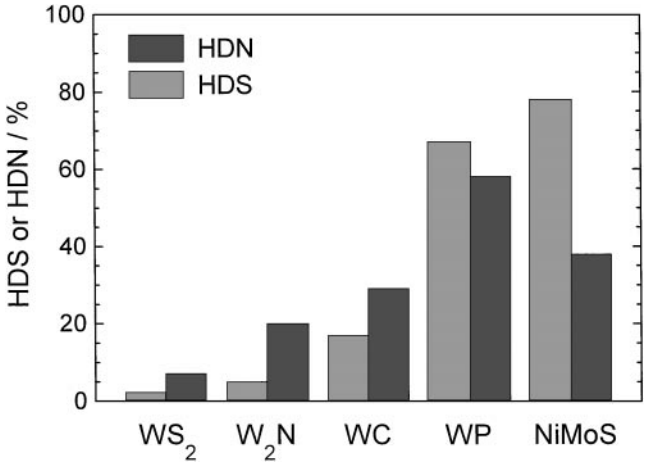

FIG. 5. Comparison of quinoline HDN and dibenzothiophene HDS conversions of WS_2, W_2N, WC, WP, and $NiMoS/Al_2O_3$ (Shell 324).

catalyst favored unsaturated biphenyl (89%), while the WS_2 yields more of the hydrogenation product cyclohexylbenzene (67%). Tetralin was found to dehydrogenate to form naphthalene under our conditions, for which WP (29%) was about three times as active as WS_2 (11%). The WP had a substantially lower cracking rate (2%) for the tetradecane solvent than the WS_2 (4%). Hexane was the most abundant alkane cracking product for each catalyst.

A comparison of the hds and hdn conversions of WP compared to WC, W_2N, WS_2, and sulfided $NiMo/Al_2O_3$ (Shell 324) is presented in Fig. 5. The conversions are directly comparable because the tests were all carried out using equal surface areas loaded in the reactors.

X-Ray Photoelectron Spectroscopy

Fresh and spent WP catalyst samples were characterized by XPS. The fresh sample was pretreated at 723 K for 2 h in hydrogen flow and then carefully passivated. The spent WP catalyst was pretreated similarly in helium flow, with the intent to desorb reactant molecules but not to remove surface sulfide (if present). The atomic concentration results are reported in Table 5. The table reveals that the catalyst sulfides only to a limited extent, having only 0.8% sulfur in the spent catalyst surface. Also, the phosphorus content of the surface region decreases slightly following catalytic reaction. Results of curve fits of the W 4*f*, W 4*d*, and P 2*p* regions are summarized in Table 6.

TABLE 5

XPS Atomic Percentage Results for Tungsten Phosphide Catalyst

	W	P	O	C	S
Fresh WP	13.2	13.5	53.7	19.5	0.0
Spent WP	13.8	12.0	48.7	24.7	0.8

TABLE 6

XPS Curve Fit Results for Tungsten 4*f* and 4*d* Regions and Phosphorus 2*p* Region

Region:	W 4*f* 7/2		W 4*d* 5/2		P 2*p* 3/2	
Sample	$W^{\delta+}$	W^{6+}	$W^{\delta+}$	W^{6+}	P°	P^{5+}
Fresh WP	31.8(15)	36.5(37)[a]	243.6(24)	247.9(76)	130.0(18)	134.6(82)
Spent WP	31.9(26)	36.8(41)[a]	244.0(26)	248.0(74)	130.1(24)	134.7(76)

Note. Binding energies are reported in keV. Relative amounts are in parentheses.

[a] Remainder of W 4*f* 7/2 region due to interference from O 1*s* singnal.

DISCUSSION

The synthesis of WP by TPR showed the presence of only one transformation feature at close to 900 K (Fig. 1) and, consistent with this, the XRD analysis of the intermediates (Fig. 2) show the growth of peaks only due to the phosphide. No features belonging to other species were observed. The final product was a phase pure tungsten monophosphide, WP (PDF 29-1364), with the MnP-type structure (space group *Pbnm*).

The oxygen to tungsten ratio of the phosphate glass precursor was calculated by the weight change of reduction to be 6.0 : 1, assuming a stoichiometric WP product. Furthermore, integration of the TPR profile reveals that ~10% of the water evolution is associated with the water of hydration. These data allow the composition of the amorphous tungsten phosphate starting material to be calculated as $WPO_{5.4} \cdot 0.6H_2O$. This agrees well with the high oxidation states expected for both tungsten and phosphorus, consisting of WO_3 and $\frac{1}{2}P_2O_5$, i.e., $WPO_{5.5}$, and matches the stoichiometry of $W_2O_3(PO_4)_2$ reported previously for tungsten phosphate (47).

As noted in Fig. 1, the *in situ* surface area of the sample increased from close to 0.1 $m^2\ g^{-1}$ for the starting material to about 11 $m^2\ g^{-1}$ for the final WP product. The removal of oxygen from the solid and the coincident increase in density accounts for the increase in surface area (48). The surface area likely decreases at higher temperatures by sintering. Estimating the density of the WP phosphate precursor as the average of P_2O_5 ($\rho = 2.39$ g cm^{-3}) and WO_3 ($\rho = 7.16$ g cm^{-3}) (49), the density increases from ~4.8 g cm^{-3} for $WPO_{5.5}$ to 8.5 g cm^{-3} for WP. The *in situ* CO uptake also passes through a maximum, tracking the changes in surface area. The *in situ* site density (ratio of CO sites to surface area) increases at high temperature, probably because of removal of residual oxygen from surface sites upon completion of the TPR peak. Still, the *in situ* site density is of the order of 6.0×10^{13} atoms cm^{-2}. This value is about an order of magnitude less than the value of 9.6×10^{14} atoms cm^{-2} (0.1037 nm^2 per W atom) calculated

from the crystal structure. This indicates that part of the surface may still be blocked by phosphorus or residual oxygen atoms.

The *ex situ* surface area and CO uptake of the catalysts are reported in Table 3. Chemisorption is thought to occur on surface vacancies, or coordinatively unsaturated sites, and has been correlated with hydroprocessing performance of materials. Typically, room temperature CO uptake is used for materials with metallic properties such as carbides and nitrides (12, 13), while dry ice/acetone temperature O_2 uptake is used for sulfides (50, 51). The O_2 chemisorption in this case is attributed to vacancies at edge sites.

In this study, hydroprocessing of quinoline and dibenzothiophene was carried out at 3.1 MPa and 643 K on 30 m^2 of WP and WS_2, the preparation and properties of which were already described. Previous studies reported the preparation and use of 30 m^2 of WC, W_2N, and $NiMoS/Al_2O_3$ for the same catalytic reaction (13, 33). Briefly, the WC and W_2N were prepared by temperature-programmed reduction of WO_3 with methane and ammonia, respectively. The commercial catalyst was presulfided at 678 K for 2 h.

Figure 4 shows the time course of reaction for WP. After a period of 30 h in which an equilibrated surface formed, the catalyst exhibited stable catalytic conversion levels until the reaction was stopped. The catalyst structure was completely stable to the reaction conditions. XRD analysis, shown in Fig. 3, demonstrates retention of all the lines belonging to WP and the lack of appearance of new peaks after reduction. Similarly, the CO uptake and BET surface area remained unchanged (Table 3) following reaction.

Figure 5 summarizes the HDS and HDN conversions of the above-mentioned samples. The tungsten phosphide is observed to be significantly more active than any other tungsten compound for both HDN and HDS and had higher HDN activity than the commercial $NiMoS/Al_2O_3$ catalyst. The catalyst also shows higher activity than MoP (28), which at the same conditions gives 33% HDN and 13% HDS.

Although the areal comparison of unsupported WP to supported NiMoS may seem to favor the phosphide, in fact the commercial catalyst is highly optimized and most of its surface area should be active. Thus, the HDN comparison based on surface area should give a good approximation of the relative activities of the materials. If, instead of surface areas, chemisorption quantities (CO for WP, and O_2 for $NiMoS/Al_2O_3$) are used for comparison, WP is calculated to be 6.9 times more active than $NiMoS/Al_2O_3$. The calculation is made as follows:

$$\frac{\text{WP}}{\text{NiMoS}} = \frac{(58\%/30\ \text{m}^2)}{(38\%/30\ \text{m}^2)} \cdot \frac{(10\ \text{m}^2\ \text{g}^{-1}/10\ \mu\text{mol g}^{-1})}{(160\ \text{m}^2\ \text{g}^{-1}/178\ \mu\text{mol g}^{-1})} = 6.9.$$

Oxygen chemisorption is known to be corrosive on sulfides, but in this case we employed a pulse technique at low temperatures which has been shown to result in just chemisorption (52, 53). Stinner *et al.* (29) recently reported that a single MoP site is 6 times more active for HDN of orthopropylaniline than alumina supported MoS_2, based on geometrical estimates of surface site density. Thus, phosphides are promising hydrotreating catalysts.

If the evaluation of activity is made on a weight basis, WP shows inferior specific rate than NiMoS in both HDN (3.1×10^{-8} vs 3.2×10^{-7} mol quinoline $g^{-1}\ s^{-1}$) and HDS (2.35×10^{-8} vs 4.37×10^{-7} mol dibenzothiophene $g^{-1}\ s^{-1}$). This is to be expected in the comparison of a bulk compound to a supported compound, and indicates the promise of the study of supported substances.

Table 5 reports the atomic concentrations on the surface of the WP catalyst before and after catalytic reaction. The data indicate the presence of substantial adventitious carbon and oxygen, as the measurements were carried out on air-exposed catalysts (carefully passivated, but not sputtered). The carbon and oxygen contamination is typical for compounds exposed to the atmosphere (12, 31).

Despite the presence of adventitious C and O, the results indicate that the P/W ratio (1.02) is close to the stoichiometric value of unity expected for the bulk compound. The phosphorus content decreases only slightly following the reaction (P/W = 0.87). There is only a small amount of sulfur on the spent catalyst surface, so the catalyst is tolerant of bulk sulfidation. The sulfur detected on the spent catalyst amounts to about 3 mol% of the surface region, counting only W, P, and S. However, since W and P analysis extends a few layers into the bulk, the S content is estimated to be larger, perhaps 10%. This small amount of sulfur may be helpful for the HDN process as adsorbed H_2S leads to both acidic (H^+) and basic (S^{2-}) surface sites, which can participate in C–N bond scission (54, 55).

Curve fits of the W 4*f*, W 4*d*, and P 2*p* regions, reported in Table 5, reveal that about 75% of the surface region is oxidized to phosphate and tungstate, and about 25% is in the reduced phosphide state. The oxidation is due to air exposure of the sample before XPS analysis. Binding energy locations reveal that the oxidation states of W and P in the WP catalyst are near elemental values (41) of 31.4 eV for the W 4*f* region, 243 eV for the W 4*d* region, and 130.0 eV for the P 2*p* region. Chemical shifts near zero have been observed for phosphides of group IV metals previously (56). We report binding energies of the W 4*d* region because of interference from the O 1*s* peak in the W 4*f* region.

Observation of oxidation of the metal and phosphorus (when present) on samples exposed to the air is common. On a nitrided Mo–P catalyst, XPS depth profiles showed mostly P 2*p* binding energy of 133.8 eV at the surface, which was attributed to phosphate bound to Mo. At much deeper layers the appearance of a small peak at 129.7 eV indicated the presence of phosphide (31).

Because of surface oxidation and carbon deposition, determination of the exact composition of the working

catalyst is difficult to establish with XPS or any other technique that is not *in situ*. The main purpose of our XPS work was to ascertain whether there was any substantial sulfidation of the surface, and the answer to this appears to be highly limited, perhaps 10 mol%.

It is likely that the oxygen content of the active catalyst is variable, given our experimental conditions. Precedence can be found in the presence of residual oxygen in typical sulfide (4), carbide (13), and nitride (12) catalysts. It was established by TPD experiments that activation at 723 K does not remove all of the oxygen from the surface region of WP. Furthermore, it is probable that the depth of the surface oxidation (passivation) layer increases with time, as the phosphide changed color from gray to black (dark blue) with aging after storage for 2 years. The effects of inclusion of oxygen in the active catalyst surface could be either positive or negative. In previous studies of hydrogenation with Ni_2P (23, 24), a beneficial interaction was identified between surface phosphorus atoms and oxygen. However, a more recent report suggests that aging due to air exposure affected amorphous nickel phosphide and boride catalysts adversely (27). The effect of air exposure on phosphide catalysts may indeed be very complicated and difficult to reproduce. Our study has been carried out with freshly prepared samples.

Although the surface P/W ratio is close to unity, the phosphorus content of the outermost layer may also be variable. One possibility is that phosphorus covers the surface region of the material similar to the way carbon covers a coked catalyst. In fact, phosphorus deposited on catalyst surfaces via the vapor phase poisoned HDS sites for all transition metals except Ni, where a promotional effect occurred (57). The other extreme in phosphorus distribution is depletion in the outermost layer, possibly by diffusion into the bulk or by vaporization from the surface region. Thus, the catalytic performance of a phosphide sample will likely depend on its preparation history. The extended soak period at 938 K used in the preparation of the WP catalyst may have helped remove trace oxygen impurities, as well as equilibrate the surface region.

Many compounds exist which contain P–S, P–C, and P–N bonds. It is conceivable that phosphorus participates in the catalytic pathway by, for example, creating P–SH sulfhydril sites. Experiments, however, showed no direct interaction between P and H_2S below 973 K (5), although this does not eliminate the possibility of metal-catalyzed interactions between heteroatoms. In addition, P/Al_2O_3 reference samples have been found to be inactive in hydroprocessing reactions (58, 59). Thus, the fundamental catalytic benefit of phosphorus in WP is likely to arise from the modification of the nature of tungsten. As mentioned earlier, sulfur on the surface also probably has a positive role in the catalytic reaction chemistry.

XPS results reveal that the oxidation states of both tungsten and phosphorus in WP are near zero. Therefore, the positive effect of alloying is likely to be based on modification of the electronic structure of the solid. One suggestion, for WC carbide reforming catalysts, was that the alloying of C and W increases the electron to atom ratio of tungsten so that its electronic structure resembles that of platinum (60). Our results do not contradict the idea that phosphorus could share its electrons with tungsten in such a way that the electronic structure of tungsten in WP is changed to be similar to noble metals adjacent on the periodic table, osmium, iridium, and platinum. The sulfides of these metals are located in the maxima in the "volcano curves" of activity for both HDN and HDS reactions (61, 62). The observed trends of HDS and HDN activities in the transition metal sulfides have also been successfully correlated by a complex combination of electronic occupation in both *d* and *p* orbitals (63).

In commercial phosphorus-promoted sulfides, phosphorus is introduced via aqueous impregnation and interacts strongly with the alumina support, in some cases forming surface $AlPO_4$ species (5, 64, 65). This leads to changes in the dispersion of the metals, for example inhibiting formation of nickel or cobalt aluminates, and encourages crystallization of bulk metal oxides such as MoO_3. Kinetic measurements have revealed that the presence of phosphorus directly affects the nature of the active sites (66, 67), and it has been suggested that the role of phosphate is to alter the nature of sites by changing the stacking of MoS_2 crystallites (68, 69). In contrast to phosphorus-promoted sulfide catalysts, where phosphorus is oxidized and associated with alumina, the phosphorus in WP is found in reduced form in the bulk.

Tungsten phosphide was highly active for both HDN and HDS reactions in coprocessing of quinoline and dibenzothiophene. The WP catalyst resisted morphology and phase changes under hydroprocessing conditions. This conclusion is common to measurements made by BET surface area, CO chemisorption, X-ray diffraction, and X-ray photoelectron spectroscopy.

CONCLUSIONS

Tungsten phosphide, WP, was prepared by reduction of an X-ray amorphous phosphate precursor with approximate composition $WPO_{5.5} \cdot 0.5H_2O$. Tungsten phosphide was highly active for hydroprocessing of quinoline and dibenzothiophene in a three-phase, fixed-bed reactor operated at 643 K and 3.1 MPa. The areal hydrodenitrogenation and hydrodesulfurization rates of WP were both superior to those found for WC, W_2N, and WS_2. The phosphorus in the bulk WP is in a reduced state, which is different from the situation with phosphorus used as a promoter in standard alumina-supported sulfide catalysts. Tungsten phosphide was stable during catalytic testing, showing no signs of bulk sulfiding, sintering, or loss of chemisorption

sites. These initial findings demonstrate that WP is one of the most active tungsten compounds yet identified for hydroprocessing reactions.

ACKNOWLEDGMENTS

This work was carried out with support from the United States Department of Energy, Office of Basic Energy Sciences, Grant DE-FG02-96ER14669.

REFERENCES

1. Minderhoud, J. K., and van Veen, J. A. R., *Fuel Process. Technol.* **35**, 87 (1993).
2. Prins, R., *in* "Characterization of Catalytic Materials" (I. E. Wachs and L. E. Fitzpatrick, Eds.), p. 109. Butterworth–Heinemann, Boston, 1992.
3. Grange, P., *Catal. Rev. Sci. Eng.* **21**, 135 (1980).
4. Furimski, E., *Catal. Rev. Sci. Eng.* **22**, 371 (1980).
5. Iwamoto, R., and Grimblot, J., *Adv. Catal.* **44**, 417 (1999).
6. Cruz Reyes, J., Avalos-Borja, M., Lopez Cordero, R., and Lopez Agudo, A., *Appl. Catal. A* **120**, 147 (1994).
7. Atanasova, P., Tabakova, T., Vladov, Ch., Halachev, T., and Lopez Agudo, A., *Appl. Catal. A* **161**, 105 (1997).
8. Atanasova, P., and Lopez Agudo, A., *Appl. Catal. B* **5**(4), 329 (1995).
9. Poulet, O., Hubaut, R., Kasztelan, S., and Grimblot, J., *Bull. Soc. Chim. Belg.* **100**, 857 (1991).
10. Callant, M., Holder, K. A., Grange, P., and Delmon, B., *Bull. Soc. Chim. Belg.* **104**, 245 (1995).
11. Oyama, S. T., Yu, C. C., and Ramanathan, S., *J. Catal.* **184**, 535 (1999).
12. Ramanathan, S., Yu, C. C., and Oyama, S. T., *J. Catal.* **173**, 1 (1998).
13. Ramanathan, S., and Oyama, S. T., *J. Phys. Chem.* **99**, 16365 (1995).
14. Danot, M., Afonso, J., Portefaix, J. L., Breysse, M., and des Couries, T., *Catal. Today* **10**, 629 (1991).
15. Cattenot, M., Portefaix, J.-L., Afonso, J., Breysse, M., Lacroix, M., and Perot, G., *J. Catal.* **173**, 366 (1998).
16. Janssens, J.-P., van Langeveld, D. A., and Moulijn, J. A., *Appl. Catal. A* **179**, 229 (1999).
17. Quartararo, J., Mignard, S., and Kasztelan, S., *J. Catal.* **192**, 307 (2000).
18. Joo, H. S., and Guin, J. A., *Fuel Process Technol.* **49**, 307 (1996).
19. Qian, W., Yoda,Y., Hirai, Y., Ishihara, A., and Kabe, T., *Appl. Catal. A* **184**, 81 (1999).
20. Cowan, R., Høglin, M., Reinink, H., Jesbaert, J., and Chadwick, D., *Catal. Today* **45**, 381 (1998).
21. Song, C., and Reddy, K. M., *Appl. Catal. A* **176**, 1 (1999).
22. Song, C., *CHEMTECH* **29**, 26 (1999).
23. Nozaki, F., and Adachi, R., *J. Catal.* **40**, 166 (1975).
24. Nozaki, F., Kitoh, T., and Sodesawa, T., *J. Catal.* **62**, 286 (1980).
25. Muetterties, E. L., and Sauer, J. C., *J. Am. Chem. Soc.* **96**(11), 3410 (1974).
26. van Veen, J. A. R., and de Beer, V. H. J., *J. Catal.* **161**, 539 (1996).
27. Lee, S.-P., and Chen, Y.-W., *J. Mol. Catal. A* **152**, 213 (2000).
28. Li, W., Dhandapani, B., and Oyama, S. T., *Chem. Lett.*, 207 (1998).
29. Stinner, C., Prins, R., and Weber, Th., *J. Catal.* **191**, 438 (2000).
30. Li, S., and Lee, J. S., *J. Catal.* **162**, 76 (1996).
31. Li, S., and Lee, J. S., *J. Catal.* **178**, 119 (1998).
32. Li, S., and Lee, J. S., *J. Catal.* **173**, 134 (1998).
33. Lucy, T., St. Clair, T., and Oyama, S. T., *J. Mater. Res.* **13**, 2321 (1998).
34. Shi, L., Wang, X. P., and Xin, Q., *Chin. Chem. Lett.* **6**(9), 819 (1995).
35. Frety, R., Breysse, M., Lacroix, M., and Vrinat, M., *Bull. Soc. Chim. Belg.* **93**(8–9), 663 (1984).
36. Vrinat, M., Lacroix, M., Breysse, M., and Frety, R., *Bull. Soc. Chim. Belg.* **93**(8–9), 697 (1984).
37. Ramanathan, K., and Weller, S. W., *J. Catal.* **95**, 249 (1985).
38. Alonso, G., Del Valle, M., Cruz, J., Licea-Claverie, A., Petranovskii, V., and Fuentes, S., *Catal. Lett.* **52**, 55 (1998).
39. Cullity, B. D., "Elements of X-Ray Diffraction," 2nd ed., p. 102. Addison–Wesley, Menlo Park, CA, 1978.
40. Falconer, J. L., and Schwartz, K. A., *Catal. Rev. Sci. Eng.* **25**, 141 (1983).
41. Moulder, J. F., Stickle, W. F., Sobol, P. E., Bomben, K. D., and Chastain, J., (Eds.), "Handbook of X-Ray Photoelectron Spectroscopy." Perkin Elmer, Eden Prairie, MN, 1992.
42. Aronsson, B., Lundstrom, T., and Rundqvist, S., "Borides, Silicides, and Phosphides," p. 65. Wiley & Sons, New York, 1965.
43. Rundqvist, S., *Acta Chem. Scand.* **16**(2), 287 (1962).
44. Tremel, W., Hoffmann, R., and Silvestre, J., *J. Am. Chem. Soc.* **108**, 5174 (1986).
45. Schönberg, N., *Acta Chem. Scand.* **8**, 226 (1954).
46. Clark, P., Ph.D. dissertation, Virginia Polytechnic Institute and State University, 2000.
47. Gopalakrishnan, J., Pandey, S., and Rangan, K. K., *Chem. Mater.* **9**, 2113 (1997).
48. Fenelonov, V. B., *kinet. Catal.* **35**(5), 736 (1994).
49. "CRC Handbook of Chemistry and Physics," 66th ed. Chemical Rubber Company, Columbus, OH, 1986.
50. Zmeirczak, W., Muralidhar, G., and Massoth, F. E., *J. Catal.* **77**, 432 (1982).
51. Bodrero, T. A., and Bartholomew, C. H., *J. Catal.* **78**, 253 (1982).
52. Millman, W. S., Bartholomew, C. H., and Richardson, R. L., *J. Catal.* **90**, 10 (1984).
53. Bodero, T. A., and Bartholomew, C. H., *J. Catal.* **84**, 145 (1983).
54. Cattenot, M., Portefaix, J.-L., Afonso, J., Breysse, M., Lacroix, M., and Perot, G., *J. Catal.* **173**, 366 (1998).
55. Yang, S. H., and Satterfield, C. N., *J. Catal.* **81**, 168 (1983).
56. Myers, C. E., Franzen, H. F., and Anderegg, J. W., *Inorg. Chem.* **242**(5), 1822 (1985).
57. Eijsbots, S., van Gestel, J. N. M., van Oers, E. M., Prins, R., van Veen, J. A. R., and de Beer, V. H. J., *Appl. Catal. A* **119**, 292 (1994).
58. Jian, M., and Prins, R., *Catal. Lett.* **35**, 193 (1995).
59. Clark, P., and Oyama, S. T., *J. Phys. Chem.*, in press.
60. Levy, R. B., and Boudart, M., *Science* **181**, 457 (1973).
61. Eijsbouts, S., de Beer, V. H. J., and Prins, R., *J. Catal.* **127**, 619 (1991).
62. Pecoraro, T. A., and Chianelli, R. R., *J. Catal.* **67**, 430 (1981).
63. Harris, S., and Chianelli, R. R., *J. Catal.* **86**, 400 (1984).
64. Morales, A., Ramirez de Agudelo, M. M., and Hernandez, F., *Appl. Catal.* **41**, 261 (1988).
65. Gishti, K., Iannibello, A., Marengo, S., Morelli, G., and Tittarelli, P., *Appl. Catal.* **12**, 381 (1984).
66. Jian, M., and Prins, R., *Catal. Today* **30**, 127 (1996).
67. Jian, M., and Prins, R., *Catal.* **179**, 18 (1998).
68. Prins, R., Jian, M., and Flechsenhar, M., *Polyhedron* **16**(18), 3235 (1997).
69. Ryan, R. C., Kemp, R. A., Smegal, J. A., Denley, D. R., and Spinnler, G. E., *Stud. Surf. Sci. Catal.* **50**, 21 (1989).